

Revisiting the 3α reaction rates in helium burning stars

T. Depastas^{a,*}, S.T. Sun^b, H.B. He^b, H. Zheng^{b,*} and A. Bonasera^{a,c}

^a Cyclotron Institute, Texas A&M University, College Station, Texas, USA

^b School of Physics and Information Technology, Shaanxi Normal University, Xi'an 710119, China

^c Laboratori Nazionali del Sud, INFN, Catania 95123, Italy

* Corresponding authors. Emails: tdepastas@tamu.edu, zhengh@snnu.edu.cn

Abstract

Helium burning is one of the most fundamental steps of stellar nucleosynthesis, as it describes the formation of life-determining element of carbon, while it plays a key role in the evolution of Red Giant, accreting White Dwarfs and Neutron Stars. In this work we develop a generalized statistical theory for the 3α reaction, which is based on the use of the Imaginary Time Method, along with the semi-classical Hybrid α -Clustering (H α C) and Neck Model (NM) frameworks. The results compared to the methodology and data of the NACRE collaboration, following in several orders of magnitude discrepancies, especially at low temperatures. This may be crucial for the early dynamics of helium burning stars.

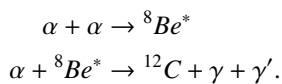
Keywords: Triple alpha reaction, Sub-barrier fusion, Imaginary Time Method, Helium Burning, Stellar Reaction Rates

In the hierarchy of stellar nucleosynthesis, carbon is produced in the helium burning stage. It takes place after the main sequence H-burning (Iliadis (2007)), at temperatures of $T \sim 10^8$ K (Rolfs and Rodney (1988)) and leads stars through the Red Giant and Asymptotic Giant Branch (AGB) phases (Hayashi et al. (1962)). It also plays a central role in more exotic phenomena, such as Type I supernovae in Neutron Stars and X-ray bursts in accreting White Dwarfs (Nomoto et al. (1985)). Its astrophysical significance has led to constraints of the reaction rates (Suda et al. (2011)), in order for results to be consistent with observations.

The mechanism of He-burning corresponds to the fusion of 3 α particles and the subsequent decay of the excited ^{12}C via sequential γ emission (Salpeter (1952)). The abundance of carbon in the universe was explained in terms of a 0^+ resonant state at $E_H = 7.654$ MeV by Hoyle (Hoyle (1954)) (the so-called ‘‘Hoyle State’’), which significantly accelerates the reaction, when compared to later burning stages, such as the $\alpha + ^{12}\text{C}$ (deBoer et al. (2017); Plag and et al. (2012); Nomoto et al. (1985); Langanke et al. (1986); Bemmerer and et al. (2011); Ogata et al. (2010); Ishikawa (2013); Angulo et al. (1999)).

We propose a theoretical framework for fusion-evaporation reactions involving charged particles and/or photons. Our results and methodology are compared to the NACRE compilation (Angulo et al. (1999); Xu et al. (2013)), also including our critical modifications to it.

The triple alpha process is given by the following two steps (Hayashi et al. (1962)):



The first step, is the fusion product of two alpha particles but into beryllium-8, which is unstable and quickly decays back into its alpha constituents, with width $\Gamma_{\alpha,\text{Be}}^{(0)} = 5.6$ eV (Angulo et al. (1999)). It is important to stress that for this process to occur the center of mass energy of the alphas must be larger than $E_{s\text{Be}} = -Q_1 = 92.08$ keV (Angulo et al. (1999)). This feature was not taken into account into the NACRE compilations and previous literature (Angulo et al. (1999); Ogata et al. (2010); Langanke et al. (1986); Ishikawa (2013)), leading to a large overestimate of the reaction rates at the lowest temperatures, as shown below. Before beryllium decays, in the second step, carbon is formed predominantly via α -fusion- γ -evaporation. It emits two E_2 photons, one from the continuum above the alpha-threshold to the 2^+ , 4.43 MeV state and one from that state to the 0^+ ground state with very small cross sections (Hayashi et al. (1962)). This results in the α and γ widths of the Hoyle state, i.e., $\Gamma_{\alpha,H}^{(0)} = 9.3$ eV and $\Gamma_{\gamma,H}^{(0)} = 5.1$ meV (Bishop et al. (2021)). The total reaction rate $R_{3\alpha}$ is written as (Angulo et al. (1999)):

$$R_{3\alpha} = \frac{\rho_\alpha^3}{3!} \langle \alpha\alpha\alpha \rangle, \quad (1)$$

where ρ_α is the number density of alphas and the reaction rate per α -triplet $\langle \alpha\alpha\alpha \rangle$ is given by:

$$N_A^2 \langle \alpha\alpha\alpha \rangle = 3N_A \sqrt{\frac{8\pi}{\mu_{\alpha\alpha} (kT)^3}} \int_{E_{s\text{Be}}}^{E_B} \frac{\hbar}{\Gamma_{\alpha,1}} \sigma_1 \{N_A \langle \sigma_2 v \rangle\} e^{-E/kT} E dE, \quad (2)$$

with $\Gamma_{\alpha,1}$ and $\sigma_1 = \sigma_{s\text{Be}}$ being the width and cross section of the first step for center of mass energy E . The quantity $N_A \langle \sigma_2 v \rangle (E^*)$ is the reaction rate per α - beryllium pair for the second step, which depends on the excitation energy of beryllium, i.e., $E^* \equiv E > E_{s\text{Be}}$. This is given by (Angulo et al.

(1999)):

$$N_A \langle \sigma_2 v \rangle (E^*) = N_A \sqrt{\frac{8\pi}{\mu_{\alpha Be} (kT)^3}} \int_0^{E_B} \sigma_2 e^{-E'/kT} E' dE', \quad (3)$$

where $\sigma_2 = \sigma_{12C}(E'; E^*)$ is the cross section for the second step. This depends both on the excitation energy of beryllium E^* and the center of mass energy of the α - beryllium pair E' , although the dependence on the former is weak, as we explain below. N_A is the Avogadro's number. We stress that the integrals are calculated from the threshold energy (E_{sBe} for step 1 and 0 MeV for step 2) up to the energy of the barrier E_B .

Since the cross sections are dominated by the 0^+ resonances of beryllium and carbon in the energy regime of interest, we adopt a statistical description for the reactions (Xu et al. (2013)). The reactant nuclei fuse creating a compound nucleus, which decays via an α or a γ channel. The cross sections are written as:

$$\sigma_{sBe}(E) = \sigma(\alpha\alpha, f), \quad (4)$$

$$\sigma_{12C}(E'; E^*) = \sigma(\alpha^8 Be, f) \frac{\Gamma_{\gamma,2}}{\Gamma_2}. \quad (5)$$

The cross sections $\sigma(\dots, f)$ describe the formation of the compound nucleus via fusion, while the branching ratio $\Gamma_{\gamma,2}/\Gamma_2$ of the widths ($\Gamma_{\gamma,2}$ gamma width and $\Gamma_2 = \Gamma_{\alpha,2} + \Gamma_{\gamma,2}$ total width) for the second step, gives the probability of the γ decay. The probability of the second γ' decay is one, since it is the only available decay channel of the 2^+ level of ^{12}C .

The fusion cross section are obtained via the use of two semi-classical models, coupled with the Feynman Path Integral method in Imaginary Time (ITM), described extensively in Refs. (Bonasera and Kondratyev (1994); Kondratyev et al. (2000); Bonasera and Natowitz (2020); Bonasera (2021); Depastas et al. (2023)). The key component of the method is the classical simulation of quantum tunneling via the evolution of the reaction system in imaginary time. This in effect reverses the sign of the collective forces below the barrier and thus, allows the system to tunnel between the classical turning points. Both the tunneling probability with relative angular momentum l , i.e., the penetrability $T_l(E_{CM})$, as well as the imaginary time interval τ , can be extracted. We note that in this study, we limit our calculations to $l = 0$, due to its dominant contribution in the low energy region. The penetrability is calculated by the action of the system in imaginary time (Kimura and Bonasera (2007); Depastas et al. (2023)), that is the integral of the imaginary momenta over the relative distance between the two turning points. The integrand values are obtained through semi-classical calculations with two different models, the Hybrid α -Clustering model (H α C) and the Neck Model (NM).

The H α C model (Zheng and Bonasera (2021)) is a dynamical description of $A = 4N_\alpha$ nuclei, with the α particles as the fundamental degrees of freedom. Their time evolution is governed by Hamiltonian equations of motion and their interaction contains a Bass nuclear potential (Bass (1977)), a Coulomb potential and a "Fermi interaction", that simulates the effect of Heisenberg and Pauli correlations of the constituents of the α particles. Due to the microscopic nature of the model, we are

able to study reactions with excited species, but we are unable to consider the effect of resonances of the compound nucleus. On the contrary, the NM (Bonasera et al. (1984)) is a macroscopic description based on the Wigner transform of the Time-Dependent Hartree-Fock densities of the reactant nuclei. The nuclei interact via the Coulomb and Bass potentials, with the latter been modified to induce resonant structures, according to the prescription of Ref. (Bonasera (2021)). The reason of using two models to calculate the fusion dynamics is their complementary characteristics. Both models give a reasonable description of fusion cross section below and above the Coulomb barrier (Depastas et al. (2023); Bonasera (2021); Bonasera and Kondratyev (1994); Bonasera et al. (1984)).

Other than the fusion cross sections, our theoretical framework requires the α and γ widths, which can be written in terms of Fermi's Golden Rule:

$$\Gamma_{\alpha/\gamma} = 2\pi |M_{\alpha/\gamma}|^2 \rho(E_{\alpha/\gamma}), \quad (6)$$

with $M_{\alpha/\gamma}$ being the matrix element and ρ the final state density of states. Following the Refs. (Gurvitz (1988); Büttiker and Landauer (1982)), the width is:

$$\Gamma_\alpha = \frac{\hbar}{\tau} T_0, \quad (7)$$

where $T_0 = \left(1 + e^{2A/\hbar}\right)^{-1}$ is the penetrability for $l = 0$ as a function of the action A in imaginary time (Bonasera and Kondratyev (1994)). No free parameters are needed in our calculations of the α - widths as function of the energy.

The γ width is given by the standard description (Ring and Schuck (1980)):

$$\Gamma_\gamma = \frac{8\pi(L+1)}{L[(2L+1)!!]^2} \left(\frac{E_\gamma}{\hbar c}\right)^{2L+1} B(E_I; L), \quad (8)$$

where L is the photon angular momentum (here $L = 2$), $E_\gamma = E_I - E_F$ is the photon energy which equals the energy difference between the initial and final levels and $B(E_I; L)$ is the reduced matrix element. Using Eq. (8) at the resonance energy $E_I = E_R$, we get easily the general formula for the γ decay width:

$$\Gamma_\gamma = \Gamma_\gamma^{(0)} \left(\frac{E_I - E_F}{E_R - E_F}\right)^{2L+1} \frac{B(E_I; L)}{B(E_R; L)}, \quad (9)$$

with $\Gamma_\gamma^{(0)}$ being the γ width at the resonance. In the literature (Xu et al. (2013); Bishop et al. (2021); Ogata et al. (2010); Angulo et al. (1999)) the last fraction in Eq. (9) is approximated to 1. This is a strong assumption implying that the matrix element is the same at the resonance (Hoyle state) and away from it. In contrast, we assume that the resonant behavior of the matrix element to be similar for both the α and γ channels. Therefore, the reduced matrix element $B(E_I; L)$ is proportional to the α matrix element, times the density of states of the compound nucleus, that is $B(E_I; L) \sim |M_\alpha|^2 \rho(E_\alpha) \sim \Gamma_\alpha$ and Eq. (9) is rewritten as:

$$\Gamma_\gamma = \Gamma_\gamma^{(0)} \left(\frac{E_I - E_F}{E_R - E_F}\right)^{2L+1} \frac{\Gamma_\alpha(E_I - Q_2)}{\Gamma_\alpha^{(0)}}, \quad (10)$$

where $Q_2 = 7.3667$ MeV (Basunia and Chakraborty (2022)) is the Q-value for the second step, $\Gamma_\alpha^{(0)}$ is the α width of the resonant state and Γ_α both given by Eq. (7).

One of the most complete and widely used methodology in the literature for calculating the astrophysical reaction rates is that of the NACRE collaboration (Angulo et al. (1999); Xu et al. (2013)). The reaction cross sections (denoted as σ^N) near the resonances are written in a Breit-Wigner form:

$$\sigma^N = \frac{\pi}{k^2} \omega_l \frac{\Gamma_i \Gamma_f}{(E - E_R)^2 + (\Gamma/2)^2}, \quad (11)$$

with ω_l a statistical factor including the spins and effects of identical nuclei, k the wavenumber of the center of mass energy E and relative angular momentum l , Γ_i , Γ_f and Γ the widths of the entrance, exit and total reaction, respectively. The cross section of the second step, is then given by:

$$\sigma_2^N = \frac{\pi}{k^2} \omega_l \frac{\Gamma_{\alpha,2} \Gamma_{\gamma,2}}{(E - E_R)^2 + (\Gamma/2)^2} \approx \frac{\pi}{k^2} \omega_l \frac{\Gamma_{\alpha,2}^2}{(E - E_R)^2 + (\Gamma_{\alpha,2}/2)^2} \frac{\Gamma_{\gamma,2}}{\Gamma_{\alpha,2}} = \sigma(\alpha^8\text{Be}, f) \frac{\Gamma_{\gamma,2}}{\Gamma_{\alpha,2}} \quad (12)$$

The difference between Eqs. (5) and (12) is striking. The denominator of the latter contains only the α width, instead of the total. For high energies, this is a more or less valid approximation, but in the limit of zero energy, the cross section is overestimated. This has important effects for the reaction rate at low temperatures, as we show later. The α and γ widths are given by (Angulo et al. (1999); Xu et al. (2013)):

$$\Gamma_\alpha = \Gamma_\alpha^{(0)} \frac{T_l(E)}{T_l(E_R)}, \quad (13)$$

$$\Gamma_\gamma = \Gamma_\gamma^{(0)} \left(\frac{E_I - E_F}{E_R - E_F} \right)^{2L+1}. \quad (14)$$

In the case of the α width, in their approach it is proportional to the penetrability and normalized to the resonant $\Gamma_\alpha^{(0)}$ value, similarly to Ref. (Lane and Thomas (1958)). In a similar manner, the γ width retains its proportionality to the fifth power of the energy and the normalization to the resonant $\Gamma_\gamma^{(0)}$. An important difference is that in the NACRE methodology, the integrals of Eqs. (2) and (3) are calculated from 0 MeV, which is not correct, because of the threshold value for ^8Be -fusion, i.e., step 1.

In Fig. 1 we plot the fusion cross sections (left) and α widths (right) as functions of E_{CM} (right). The NACRE cross sections are smaller than the H α C and NM (apart at the resonance). We also notice that our calculated cross sections correctly start from $E_{s\text{Be}}$ while the NACRE results do not.

The calculated widths (NM) are similar with the corresponding experimental values (Angulo et al. (1999); Bishop et al. (2021)) (black points). Also, we plot the widths with the NACRE formulas Eq. (14) using two penetrability formulas, the one from the ITM which accounts for both the Coulomb and Nuclear potentials (see Ref. Depastas et al. (2023)) and the other from the quantum mechanical Coulomb scattering (see

Ref. Xu et al. (2013)). We stress that the widths calculated from Eq. (8), are resulting purely by the sub-barrier nuclear dynamics in imaginary times. On the contrary, in Ref. (Angulo et al. (1999)) the normalization to the resonant value, results in much higher widths for the entire energy region.

We present the results of the $(\alpha, \gamma\gamma')$ cross sections for

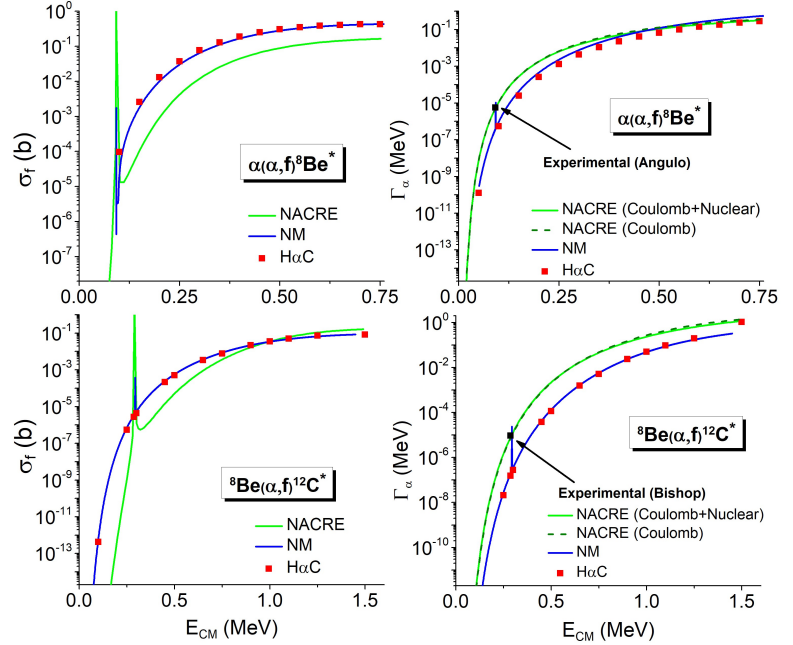


Figure 1: (Color online) Fusion cross sections (left column) and α widths (right column) for the $\alpha(\alpha, f)^8\text{Be}^*$ (top) and $^8\text{Be}(\alpha, f)^{12}\text{C}^*$ (bottom). The results of NACRE (Angulo et al. (1999)), H α C and NM are given according to the key. The experimental widths (Angulo et al. (1999); Bishop et al. (2021)) are noted by black points.

different excitation energies in Fig. 2. On the top panel the data for the fusion of the beryllium ground state are shown, while on the bottom panel the results for $E^* = 0.10, 0.50$ and 0.75 MeV are given. The NACRE cross sections are smaller, while the $\Gamma_\gamma/\Gamma_\alpha$ and Γ_γ/Γ formulas Eqs. (5) and (12) differ only in the low energy region, as expected. The NM and H α C results are similar, apart from the resonance not included in the H α C model. The γ widths given by Eq. (14), are normalized to their resonant values, which leads to higher values of Γ_γ than the NACRE data.

On the bottom panel, we see that the cross sections of the H α C model are almost independent of the excitation energy of the beryllium. This allows us to factor out the $N_A \langle \sigma_2 v \rangle$ rate from the integral in Eq. (2). In the case of the H α C model, we take this to be equal to an average rate plus an error, both resulting from the data of Fig. 2, i.e., $N_A \langle \sigma_2 v \rangle(E^*) \rightarrow N_A (\langle \sigma_2 v \rangle \pm \delta \langle \sigma_2 v \rangle)$. For the NM, we use the ground state rate, i.e., $N_A \langle \sigma_2 v \rangle(E^*) \rightarrow N_A \langle \sigma_2 v \rangle(E^* = 0 \text{ MeV})$.

Finally, we present the stellar reaction rates according to Eq. (2) in Fig. 3 (top). There we show the H α C (red) and NM (blue) calculations, the original NACRE (green) (Angulo et al. (1999)), as well as the NACRE with the corrections of widths and threshold energies (black). These corrections consist of using the width ratio $\Gamma_{\gamma,2}/\Gamma_2$ instead of $\Gamma_{\gamma,2}/\Gamma_{\alpha,2}$ in

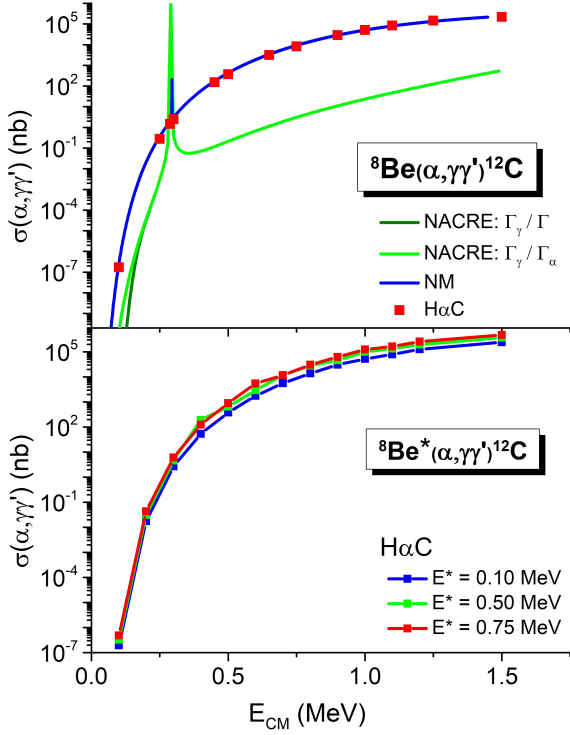


Figure 2: (Color online) The cross section for the ${}^8\text{Be}(\alpha, \gamma\gamma'){}^{12}\text{C}$ reaction, with the beryllium in its ground state (top) and in the excited continuum (bottom). The results of NACRE in its original form (Angulo et al. (1999)) and with the width correction, as well as the data from the H α C and NM calculations, are given according to the key.

Eq. (12) and integrating the reaction rates from the threshold energy $E_{8\text{Be}}$ instead from 0 MeV, similarly to Eq. (2). In the middle panel, we re-plot the same quantities normalized by the corresponding corrected NACRE values. On the bottom panel, we illustrate the temperature dependence ν of the reaction rate, defined in the figure.

We observe that the original NACRE prescription has an enhanced rate by almost 20-30 orders of magnitude for temperatures $T \sim 10^7$ K, when compared to the other approaches (Ogata et al. (2010); Ishikawa (2013); Nguyen et al. (2013); Bemmerer and et al. (2011)). This may also have significant consequences for stellar dynamics, since the helium burning may start prematurely in stars of lower temperature than $T \sim 10^{7.6}-10^8$ K (Suda et al. (2011)), as discussed in the literature. We emphasize that the H α C results are lower than the other approaches, due to the lack of resonant peaks, while the NM data are higher than the corrected NACRE and the H α C, due to the existence of such structures and the increased γ cross section (as shown in Fig. 2).

In the top panel of Fig. 3, we also include an astrophysical upper limit by Suda *et. al* (Suda et al. (2011)). This limit restricts the maximum reaction rate at $T \sim 10^{7.8}$ K to the value of $10^{-29} \text{ cm}^6 \text{ s}^{-1} \text{ mol}^{-2}$. The constraint comes from the requirement that the helium ignition takes place at high enough temperature in order for the First Asymptotic Giant Branch (FBG) stars to have a value of luminosity in agreement to observations.

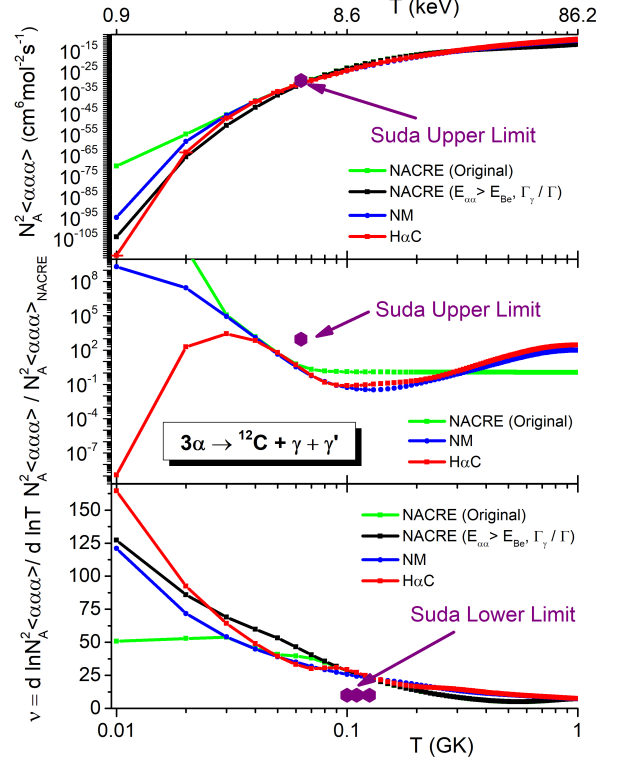


Figure 3: (Color online) The reaction rate per α triplet according to Eq. (2) (top), the same quantity normalized by the corrected NACRE data (middle) and the temperature dependence (bottom). The original (Angulo et al. (1999)) and corrected NACRE data, as well as the H α C and NM results are shown, according to the key. We also emphasize the astronomical constraints by Suda *et. al* (Suda et al. (2011)) with purple points.

Apart from the upper rate constraint, Suda *et. al* (Suda et al. (2011)) proposed a lower limit in the temperature dependence ν . Specifically, $\nu \gtrsim 10$ in the region $T \sim 10^8 - 1.2 \cdot 10^8$ K. This requirement ensures that Asymptotic Giant Branch (AGB) stars experience helium flashes on their shells, which result in third dredge-up events that explain the presence of S-process elements such as ${}^{99}\text{Tc}$ in their outer envelopes (Suda et al. (2011)). Thus, more stringent constraints are required for the helium burning rates and these might come from Nuclear Physics. Studies could be performed through the utilization of the Trojan Horse Method (THM) (Tumino et al. (2018)), which is able to effectively bypass the issue of the small life time of beryllium-8 and the suppression of the cross section due to Coulomb interaction, via the use of a heavier clustered nuclear system (see Fig. 2, top).

To summarize, we developed a theoretical framework for the low energy astrophysical fusion-evaporations involving charged particles and/or photons based on the statistical breakup of a compound nucleus, formed through the tunneling of the reactant system. The fusion cross sections are calculated via the Feynman Path Integral method in Imaginary Time, coupled with the semi-classical H α C and NM models. We furthermore derive approximate formulas for the charged particle and photon widths.

For the 3α process and we find results consistent with both

nuclear and astrophysical constraints. Finally, we note the need for stringer constraints of the functional form of cross sections and we propose possible experimental investigations with the Trojan Horse Method.

ACKNOWLEDGEMENTS

This work was supported in part by the United States Department of Energy under Grant #DE-FG03-93ER40773, NNSA Grant No. DENA0003841 (CENTAUR) and by the National Natural Science Foundation of China (Grant Nos. 11905120 and 11947416).

References

- Angulo, C., Arnould, M., Rayet, M., Descouvemont, P., Baye, D., Leclercq-Willain, C., Coc, A., Barhoumi, S., Aguer, P., Rolfs, C., Kunz, R., Hammer, J., Mayer, A., Paradellis, T., Kossionides, S., Chronidou, C., Spyrou, K., Degl'Innocenti, S., Fiorentini, G., Ricci, B., Zavatarelli, S., Providencia, C., Wolters, H., Soares, J., Grama, C., Rahighi, J., Shotter, A., Laméhi Rachti, M., 1999. *Nuclear Physics A* 656, 3–183.
- Bass, R., 1977. *Phys. Rev. Lett.* 39, 265.
- Basunia, M., Chakraborty, A., 2022. *Nucl. Data Sheets* 186.
- Bemmerer, E., et al., 2011. *Eur. Phys. J. A* 47, 102.
- Bishop, J., Rogachev, G.V., Ahn, S., Aboud, E., Barbui, M., Bosh, A., Hooker, J., Hunt, C., Jayatissa, H., Koshchiy, E., Malecek, R., Marley, S.T., Munch, M., Pollacco, E.C., Pruitt, C.D., Roeder, B.T., Saastamoinen, A., Sobotka, L.G., Upadhyayula, S., 2021. *Phys. Rev. C* 103, L051303.
- Bonasera, A., 2021. *EPJ Web Conf.* 252, 05001.
- Bonasera, A., Bertsch, G., El-Sayed, E., 1984. *Phys. Lett. B* 141.
- Bonasera, A., Kondratyev, V., 1994. *Phys. Lett. B* 339, 207–210.
- Bonasera, A., Natowitz, J.B., 2020. *Phys. Rev. C* 102, 061602.
- Büttiker, M., Landauer, R., 1982. *Phys. Rev. Lett.* 49, 1739–1742.
- deBoer, R.J., Görres, J., Wiescher, M., R.E. Azumaand Best, A., Brune, C.R., Fields, C.E., Jones, S., Pignatari, M., Sayre, D., Smith, K., Timmes, F.X., Uberseder, E., 2017. *Rev. Mod. Phys.* 89, 035007.
- Depastas, T., Sun, S.T., Zheng, H., Bonasera, A., 2023. *Phys. Rev. C* 108, 035806.
- Gurvitz, S., 1988. *Phys. Rev. A* 38, 1747–1759.
- Hayashi, C., Hōshi, R., Sugimoto, D., 1962. *Progress of Theoretical Physics Supplement* 22, 1–183.
- Hoyle, F., 1954. *Astrophys. J. Suppl.* 1, 121.
- Iliadis, C., 2007. *Nuclear Physics of Stars*. Wiley, Weinheim.
- Ishikawa, S., 2013. *Phys. Rev. C* 87, 055804.
- Kimura, S., Bonasera, A., 2007. *Phys. Rev. C* 76, 031602.
- Kondratyev, V., Bonasera, A., Iwamoto, A., 2000. *Phys. Rev. C* 61, 044613.
- Lane, A.M., Thomas, R., 1958. *Rev. Mod. Phys.* 30, 257–353.
- Langanke, K., Wiescher, M., Thielemann, F., 1986. *Z. Physik A - Atomic Nuclei* 324, 147–152.
- Nguyen, N., Nunes, F., Thompson, I., 2013. *arXiv:1209.4999*.
- Nomoto, K., Thielemann, F.K., Miyaji, S., 1985. *Astron. Astrophys.* 149, 239–245.
- Ogata, K., Kan, M., Kamimura, M., 2010. *AIP Conference Proceedings* 1269, 268–275.
- Plag, R., et al., 2012. *Phys. Rev. C* 86, 015805.
- Ring, P., Schuck, P., 1980. *The nuclear many-body problem*. Springer-Verlag, New York.
- Rolfs, C.E., Rodney, W.S., 1988. *Cauldrons in the cosmos: Nuclear astrophysics*. University of Chicago press.
- Salpeter, E.E., 1952. *Astrophys. J.* 115, 326–328.
- Suda, T., Hirschi, R., Fujimoto, M., 2011. *The Astrophysical Journal* 741, 61.
- Tumino, A., Spitaleri, C., Cognata, M.L., Cherubini, S., Guardo, G.L., Gulino, M., S. Hayakawa, I.I., Lamia, L., Petrascu, H., Pizzone, R.G., Puglia, S.M.R., Rapisarda, G.G., Romano, S., Sergi, M.L., Spartá, R., Trache, L., 2018. *Nature* 557, 687–690.
- Xu, Y., Takahashi, K., Goriely, S., Arnould, M., Ohta, M., Utsunomiya, H., 2013. *Nuclear Physics A* 918, 61–169.
- Zheng, H., Bonasera, A., 2021. *Symmetry* 13, 1777.